Journal of Solid State Chemistry 182 (2009) 1899–1906

Contents lists available at ScienceDirect

Journal of Solid State Chemistry

journal homepage: www.elsevier.com/locate/jssc

Synthesis, crystal structures and properties of three new mixed-ligand d^{10} metal complexes constructed from pyridinecarboxylate and *in situ* generated amino-tetrazole ligand

Dongsheng Liu [a,b], Xihe Huang [a], Changcang Huang [a,*], Gansheng Huang [a,b], Jianzhong Chen [a,*]

[a] State Key Laboratory Breeding Base of Photocatalysis, College of Chemistry and Chemical Engineering, Fuzhou University, Fuzhou, Fujian 350108, PR China
[b] College of Chemistry and Chemical Engineering, Jinggangshan University, Ji'an, Jiangxi 343009, PR China

ARTICLE INFO

Article history:
Received 26 February 2009
Received in revised form
29 April 2009
Accepted 30 April 2009
Available online 10 May 2009

Keywords:
5-Amino-tetrazolate
In situ
Mixed-ligand
Crystal structure
Properties

ABSTRACT

Three new metal–organic frameworks, $[Zn(atz)(nic)]_n$(1), $[Zn(atz)(isonic)]_n \cdot n$Hisonic(2) and $[Cd(atz)(isonic)]_n$(3) (Hnic = nicotinic acid, Hisonic = isonicotinic acid), have been firstly synthesized by employing mixed-ligand of pyridinecarboxylate with the *in situ* generated ligand of 5-amino-tetrazolate(atz^-), and characterized by elemental analysis, IR spectroscopy, TGA and single crystal X-ray diffraction. The results revealed that **1** presents a two-dimensional (2D) "sql" topological network constructed from the linear chain subunit of $Zn(nic)_2$ and atz^- ligand. A remarkable feature of **2** is a 2-fold interpenetrated diamondoid network with free Hisonic molecules locating in the channels formed by the zigzag chain subunits of $Zn(isonic)_2$. Complex **3** is a 3D non-interpenetrated pillared framework constructed from the double chain subunits of Cd–COO^-–Cd. It possesses a rarely observed (4,6)-connected "*fsc*" topology. The thermal stabilities and fluorescent properties of the complexes were investigated. All of these complexes exhibited intense fluorescent emissions in the solid state at room temperature.

1. Introduction

In recent years a new research field has been developed in the tetrazole chemistry, coordination complexes containing a tetrazole group have been the subject of an intense research effort due to their variety of intriguing architectures and their potential applications in advanced materials [1,2]. Numerous metal–organic coordination complexes constructed from tetrazole-based ligand have been reported, such as the low-dimensional structures of transition metal complexes of tetrazolate and derivatives (1-*R*-tetrazoles), *R* = alkyl [3–5], phenyl [6,7], chloroethyl [8–10] and methoxyethyl [11] etc. However, the unfunctionalized substituents show no coordination ability and thus disfavor the formation of highly extended structures. In order to construct high-dimensional metal–tetrazolate materials, a good synthetic strategy is to utilize different functional groups to functionalized-substitute tetrazolate. Thanks to the pioneering work of Demko & Sharpless, tetrazole-based ligands can be obtained by an environmentally friendly process [12,13]. Many functionalized-substituted tetrazoles and derivatives have been produced such as pyridyl-tetrazole (PTZ), pyrimidyl-tetrazole (PMTZ) carboxylate-tetrazole, bistetrazole (BTZ), and aminotetrazole (ATZ) etc., and several extended high-dimensional metal–organic coordination complexes [14–26] have been synthesized and structurally characterized. In recent research, chemists have concentrated on the construction of mixed-ligand MOFs based on triazolate-system and carboxylate species and got some unique 3D architectures or 2-fold interpenetrating layered networks [27–30]. These results reveal that the mixed-ligand synthetic approach is reliable to achieve unusual MOFs.

Nicotinic acid and isonicotinic acid, as good sources of carboxylate ligand, have been wildly applied to construct MOFs. We apply nicotinic or isonicotinic acid in the tetrazole-based system as a second ligand based on the following considerations: (i) nicotinic acid and isonicotinic acid are positional isomers with both N and O donor atoms. They have been proven to be able to form novel structures with different metal ions [31–35]; (ii) nicotinic acid and isonicotinic acid, the difference in the coordination orientation of the two binding sites, py and carboxylate groups, straight for isonic, and bent for nic, would affect the crystal structure and properties of a complex. While compared with those reported metal–tetrazolate cases, mixed-ligand coordination complexes with tetrazole and carboxylic acid

* Corresponding authors.
E-mail addresses: changcanghuang@hotmail.com (C.C. Huang), j.z.chen@fzu.edu.cn (J.Z. Chen).

0022-4596/$ - see front matter © 2009 Elsevier Inc. All rights reserved.
doi:10.1016/j.jssc.2009.04.034

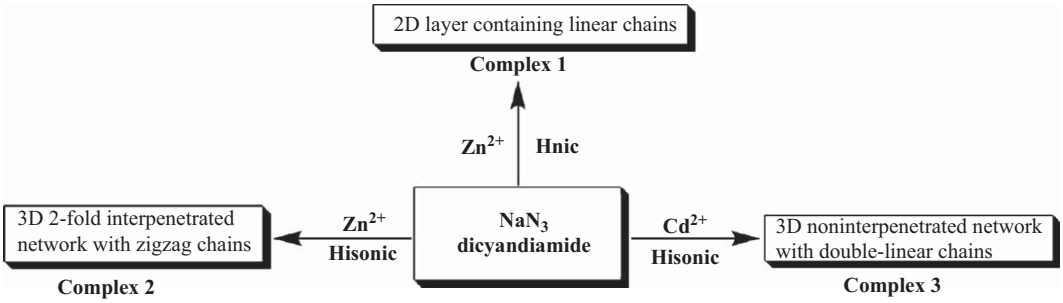

Scheme 1.

ligands are rarely presented up to now. Herein we report three new complexes $[Zn(atz)(nic)]_n$(1), $[Zn(atz)(isonic)]_n \cdot n$Hisonic (2) and $[Cd(atz)(isonic)]_n$(3) (Hnic = nicotinic acid, Hisonic = isonicotinic acid), which were constructed from the reaction of Zn^{2+} (or Cd^{2+}) with mixed-ligand of pyridinecarboxylate and the *in situ* generated ligand of 5-amino-tetrazolate. The thermal stabilities and photoluminescence properties of the complexes have also been studied.

2. Experimental section

2.1. Reagents and physical measurements

All reagents and solvents employed were commercially available and used as received without further purification. Infrared spectra were recorded in the range 4000–400 cm^{-1} on a Perkin-Elmer FT-IR spectrum 2000 spectrometers using KBr pellets. Elemental analyses were determined with a Perkin-Elmer model 240C instrument. The fluorescent spectra were recorded on an Edinburgh Instrument FL/FS-920 fluorescent spectrometer. Thermal analyses were performed on a Delta Series TGA7 instrument in N_2 atmosphere with heating rate of 10 °C min from 40 to 900 °C.

2.2. Synthesis of $[Zn(atz)(nic)]_n$(1)

A mixture of $Zn(NO_3)_2 \cdot 6H_2O$ (0.2975 g, 1.0 mmol), NaN_3 (0.0325 g, 0.5 mmol), DCDA (DCDA = dicyandiamide, 0.042 g, 0.5 mmol), Hnic (0.122 g, 1.0 mmol) ethanol (2 ml) and water (8 ml) was stirred for 30 min in air (Scheme 1), then sealed in a 23 ml Teflon autoclave and heated at 130 °C for 3 days. After the sample was cooled to room temperature at a rate of 10 °C/h, colorless lamellar crystals were obtained in ca. 38% yield based on Zn. Anal. found: C, 31.03%; H, 2.21%; N, 30.91%. Calcd for $Zn_2C_{14}H_{12}N_{12}O_4$ (MW = 543.10): C, 30.96%; H, 2.23%; N, 30.95%.

2.3. Synthesis of $[Zn(atz)(isonic)]_n \cdot n$(Hisonic)(2)

The hydrothermal procedure for the preparation of complex **2** is similar to that for **1** except by replacement of Hnic with Hisonic. Colorless pillar crystals were obtained in ca. 46% yield based on Zn. Anal. found: C, 35.53%; H, 2.21%; N, 28.81%. Calcd for $ZnC_{10}H_8N_7O_3$ (MW = 339.60): C, 35.36%; H, 2.37%; N, 28.87%.

2.4. Synthesis of $[Cd(atz)(isonic)]_n$(3)

Similarly, complex **3** was prepared in the same manner as that for **2** but with $Cd(NO_3)_2 \cdot 2H_2O$ to replace $Zn(NO_3)_2 \cdot 6H_2O$. Colorless pillar crystals were obtained in ca. 46% yield based on Cd. Anal. found: C, 26.41%; H, 1.88%; N, 26.31%. Calcd for $CdC_7H_6N_6O_2$ (MW = 318.58): C, 26.39%; H, 1.90%; N, 26.38%.

Table 1
Crystal data and structure refinement for complexes **1**–**3**.

Complex	1	2	3
Empirical formula	$C_{14}H_{12}N_{12}O_4Zn_2$	$C_{10}H_8N_7O_3Zn$	$C_7H_6N_6O_2Cd$
Formula weight	543.10	339.60	318.58
Temperature(K)	298(2)	298(2)	298(2)
Crystal system	Orthorhombic	Monoclinic	Orthorhombic
Space group	*Pbca*	*C2/c*	*Pbcm*
a (Å)	13.901(3)	17.160(3)	9.795(2)
b (Å)	9.3017(19)	16.787(3)	6.7576(14)
c (Å)	15.672(3)	10.072(2)	13.220(3)
α (deg)	90.00	90.00	90.00
β (deg)	90.00	120.77(3)	90.00
γ (deg)	90.00	90.00	90.00
V (Å^3)	2026.5(7)	2493.0(9)	875.1(3)
Z	4	8	4
D_{cal} (g/cm^3)	1.780	1.810	2.418
μ(Mo *K*α) (mm^{-1})	2.419	1.994	2.490
F(000)	1088	1368	616
2θ (deg)	3.66, 26.36	3.38 , 27.10	3.08, 27.52
Reflections collected	13775	9618	6501
Independent reflections	2064	2748	1057
Data completeness	0.998	0.997	0.999
Data/restraints/parameters	2064/0/170	2748/0/216	1057/0/91
Goodness-of-fit on F^2	1.479	1.138	1.289
*R*1, w*R*2 [$I>2\delta(I)$]	0.0797, 0.1109	0.0360, 0.0820	0.0325, 0.0781
*R*1, w*R*2 [all data]	0.0848, 0.1125	0.0390, 0.0834	0.0333, 0.0785
Max peak (hole/e Å^3)	0.323, −0.261	0.436, −0.561	0.507, −0.584

2.5. X-ray crystallographic determination

Suitable single crystals of three complexes were mounted on glass fibers for X-ray measurement. Reflection data were collected at room temperature on a Rigaku Saturn 724 CCD diffractometer with graphite monochromatized Mo *K*α radiation($\lambda = 0.71073$ Å). Crystal structures were solved by the direct method and different Fourier syntheses. All calculations were performed using the SHELX-97 program [36]. All non-hydrogen atoms were refined by full-matrix least-squares techniques on F^2 with anisotropic thermal parameters. The hydrogen atoms were fixed at calculated positions and refined by using a riding mode. In complex **2**, the free Hisonic ligand is disordered in two reversed directions. Crystal data and details of the data collection and the structure refinement are given in Table 1. Selected bond lengths and bond angles of the complexes are listed in Table 2.

Table 2
Selected bond lengths (Å) and angles (deg) for **1**, **2**, and **3**.

Complex **1**[a]			
Zn(1)–N(2)♯1	1.996 (5)	Zn(1)–O(1)♯2	1.999 (4)
Zn(1)–N(5)	2.009 (5)	Zn(1)–N(6)	2.048 (4)
N(2)♯1–Zn(1)–O(1)♯2	112.7 (2)	N(2)♯1–Zn(1)–N(5)	102.02 (19)
O(1)♯2–Zn(1)–N(5)	129.49 (19)	N(2)♯1–Zn(1)–N(6)	107.88 (18)
O(1)♯2–Zn(1)–N(6)	99.97 (16)	N(5)–Zn(1)–N(6)	102.95 (19)
Complex **2**[b]			
Zn(1)–O(1)	1.9480 (19)	Zn(1)–N(5)	1.975 (2)
Zn(1)–N(2)♯1	1.992 (2)	Zn(1)–N(6)♯2	2.044 (2)
O(1)–Zn(1)–N(5)	120.60 (9)	O(1)–Zn(1)–N(2)♯1	113.29 (9)
N(5)–Zn(1)–N(2)♯1	109.68 (10)	O(1)–Zn(1)–N(6)♯2	97.76 (9)
N(5)–Zn(1)–N(6)♯2	106.96 (9)	N(2)♯1–Zn(1)–N(6)♯2	106.81 (9)
Complex **3**[c]			
Cd(1)–N(3)	2.254 (3)	Cd(1)–N(3)♯1	2.254 (3)
Cd(1)–O(1)♯2	2.419 (3)	Cd(1)–O(1)♯3	2.419 (3)
Cd(1)–N(1)♯4	2.504 (4)	Cd(1)–O(1)	2.635 (3)
N(3)–Cd(1)–N(3)♯1	169.81 (16)	N(3)–Cd(1)–O(1)♯2	90.57 (11)
N(3)♯1–Cd(1)–O(1)♯2	89.91 (11)	O(1)♯2–Cd(1)–O(1)♯3	174.62 (12)
O(1)♯2–Cd(1)–O(1)	67.36 (10)	N(3)♯1–Cd(1)–N(1)♯4	84.91 (8)
N(1)♯4–Cd(1)–O(1)	155.29 (6)	O(1)♯3–Cd(1)–N(1)♯4	92.69 (6)
N(3)♯1–Cd(1)–O(1)♯1	81.05 (10)	N(3)♯1–Cd(1)–O(1)	108.48 (11)
O(1)♯3–Cd(1)–O(1)	107.45 (7)		

Symmetry codes (a):♯1 $-x+1/2, y+1/2, z$. ♯2 $x, -y+1/2, z+1/2$, ♯3 $-x+1/2, -y, z+1/2$; symmetry codes (b): ♯1 $x, -y, z+1/2$. ♯2 $x-1/2, -y+1/2, z-1/2$, ♯4 $x, -y, z-1/2$; and symmetry codes (c): ♯1 $x, -y+1/2, -z+1$ ♯2 $-x, -y, -z+1$ ♯3 $-x, y+1/2, z$. ♯4 $x+1, y, z$.

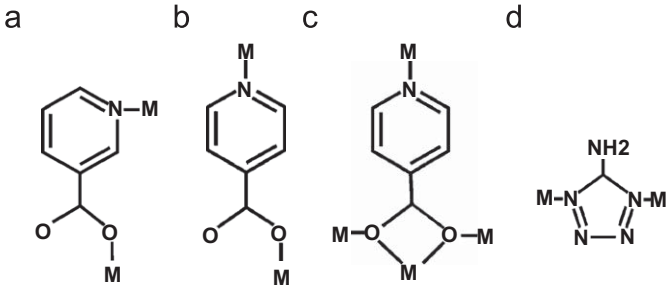

Chart 1. Coordination fashions of nic, isonic and atz ligands in this paper.

3. Results and discussion

3.1. Synthesis

Hydrothermal reaction (130 °C) of NaN_3, dicyandiamide, Hisonic, ethanol and $Zn(NO_3)_2 \cdot 6H_2O$ (for 2), or $Cd(NO_3)_2 \cdot 2H_2O$ (for 3) in water in different molar ratios yielded $[Zn(atz)(isonic)]_n \cdot n$(Hisonic)(2), $[Cd(atz)(isonic)]_n$(3). While the corresponding reactions of dicyandiamide with NaN_3 and $Zn(NO_3)_2 \cdot 6H_2O$ (or $Cd(NO_3)_2 \cdot 2H_2O$) in the replacement of Hisonic with Hnic gave $[Zn(atz)(nic)]_n$(1), but failed in preparing the complex of Cd with nic and atz, only led to white powder, although the reaction temperature was changed from 100 to 180 °C.

3.2. Crystal structure of complex 1

The different coordination modes of the nic, isonic and atz ligands in the three complexes are listed in Chart 1a–d.

Single crystal X-ray analysis shows that complex **1** is a 2D square lattice structure. There is one four-coordinated Zn(II) atom, one nic ligand, and one atz ligand in the asymmetric unit, of which the Zn(II) atom, nic and atz ligands are all sited in the general position (Fig. 1a). The Zn(II) ion is coordinated with three nitrogen atoms from two bridging μ_2-atz$^-$ ligands (N5 and N2(i))

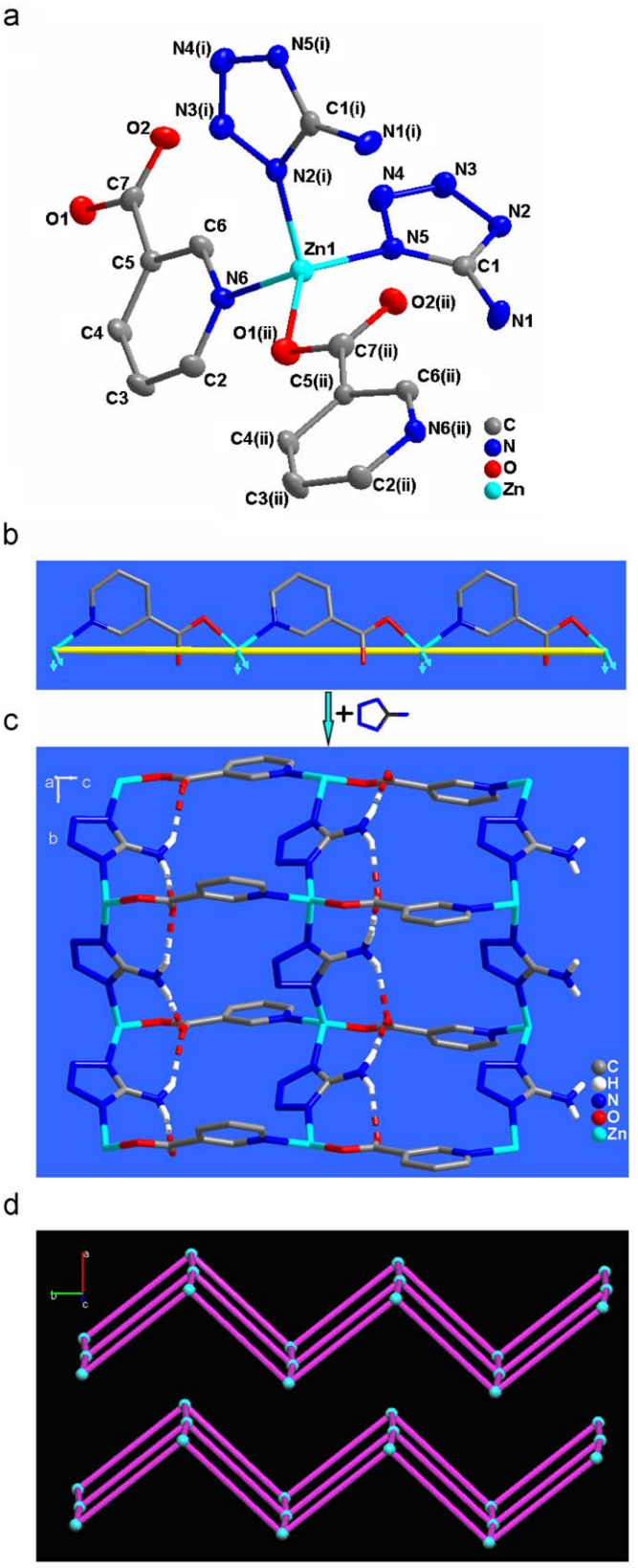

Fig. 1. (a) View of the coordination environment of Zn^{2+} in complex **1** at 30%, Hydrogen atoms are omitted for clarity. Symmetry codes: (i) $0.5-x, 0.5+y, z$ and (ii) $x, 0.5-y, 0.5+z$. (b) View of the Zn–Zn linear chain connected by the bridging nic ligands (arrowhead for Zn atoms indicating the coordination direction). (c) View of the wavy 2D layer structure constructed from Zn–Zn linear chains and atz$^-$ ligands. (d) Topological view of the 2D 4-connected topological network with the Schläfli symbol of $4^4 \cdot 6^2$ networks. Zn nodes are represented by cyan balls.

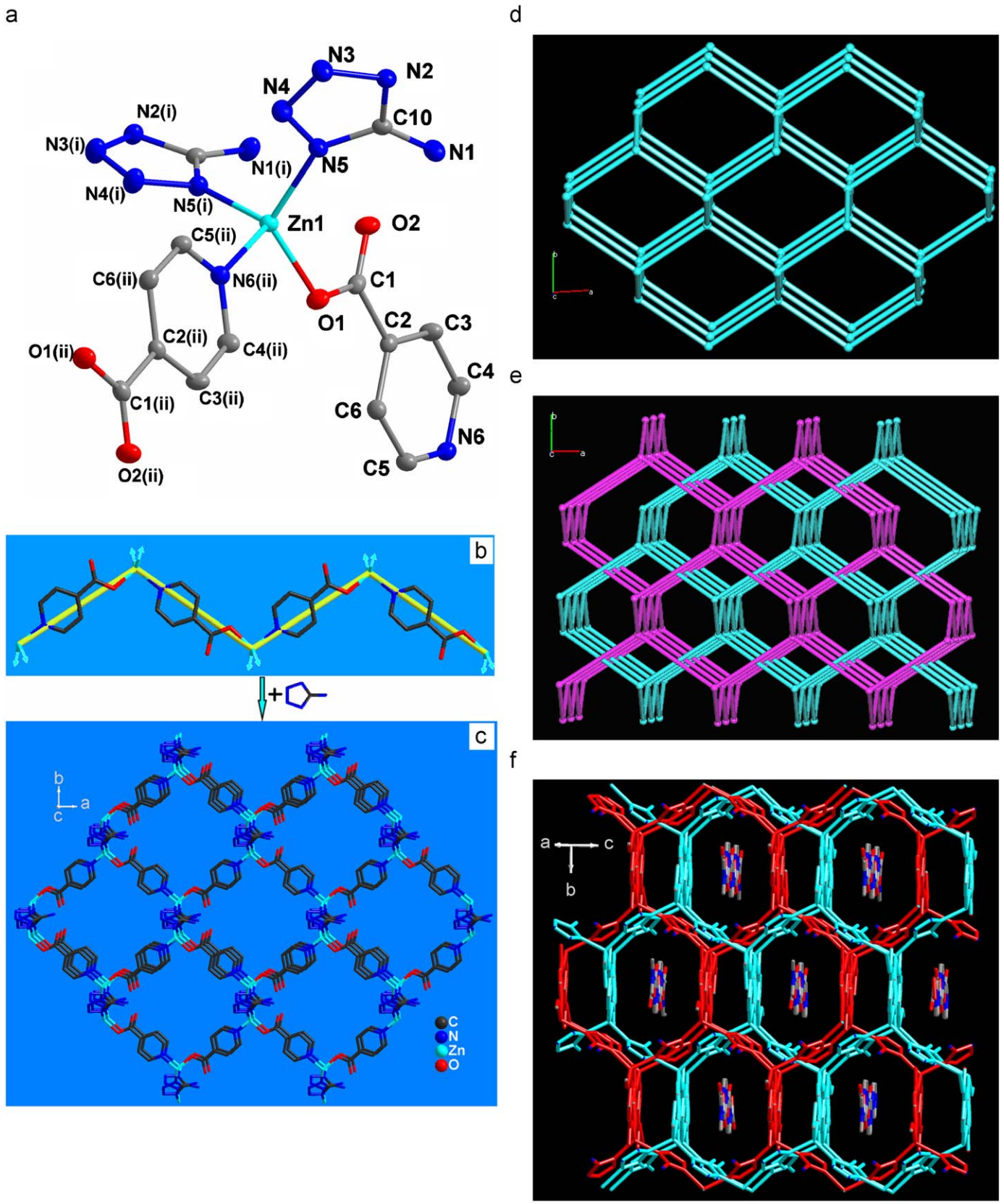

Fig. 2. (a) View of the coordination environment of Zn^{2+} in complex **2** at 30%, Hydrogen atoms are omitted for clarity. Symmetry codes: (i) $x, -y, 0.5+z$ and (ii) $-0.5+x, 0.5-y, -0.5+z$. (b) View of the Zn–Zn zigzag chain connected by the bridging isonic ligands (arrowhead for Zn atoms indicating the coordination direction). (c) View of the single 3D network constructed from the Zn–Zn zigzag chains and the atz^- ligands. (d) Topological view showing the individual diamondoid network for complex **2** along approximate [001] direction with the Schläfli symbol of 66 network. Zn nodes are represented by cyan balls. (e) View of the 2-fold-interpenetrated 3D topological network for 2 constructed from two identical diamondoid net along *c*-axis. Zn nodes are represented by cyan and purple balls. (f) View of the 2-fold interpenetration 3D network for complex **2** including free Hisonic in the cavities. The hydrogen atoms are omitted for clarity.

and one nic ligand (N6) (Chart 1a and d), one monodentate carboxylate group oxygen atom (O1(ii)) from the other inic groups, to form a slightly distorted ZnN_3O tetrahedron with the cis-bond angles ranging from 102.0(2)–112.7(2)°. The bond length of Zn–N range from 1.995(5)–2.048(5) Å, Zn1–O1(ii) bond length is 1.999(4) Å. All the Zn–N and Zn–O bond lengths are comparable to those of the Zn(II)–tetrazole and the Zn(II)–nicotinate compounds.

In this structure, the ZnN_3O tetrahedra are bridged into a linear chain by μ_2-nic$^-$ (N,O) ligand along the *bc* plane (Fig. 1b), then the linear chains are linked into wavy 2D layer by the μ_2-atz$^-$ ligand along the *b*-axis (Fig. 1c) direction and formed a "sql" topology with the Schläfli symbol [37] of $4^4\cdot6^2$ and the vertex symbol or long symbol [38], of $4\cdot4\cdot4\cdot4\cdot6^2\cdot6^2$ (Fig. 1d). The wavy 2D layers are stabilized by the weak intralayer N–H…O hydrogen bonding interactions (N1–H3…O2(♯3), 2.915 Å N1–H6…O2(♯2), 2.928 Å), via the amino groups donating H atoms to the uncoordinated carboxylate oxygen atoms (Fig. 1c). The layers further pack along [100] direction into a 3D supramolecular structure via weak $\pi\ldots\pi$ stacking interaction between the neighboring pyridyl ring of two nic ligands (Figure S1, Supporting information). The two adjacent pyridyl rings are paralleling to each other with a distance of 3.906(3) Å and slight offset (the centroid-to-centroid distance of the two pyridyl rings is 3.954(1) Å. Compared with the similar structure reported by Xiong's group [26], the size of square grid Zn–Zn–Zn–Zn increased effectively via the nic ligand replacement of the OH$^-$group. The distances between Zn–Zn are 7.837 and 6.143 Å in complex **1** much larger than that distances of 3.369 and 6.105 Å in the reported case. Another most different feature of the two comparable complexes is, interestingly, all of the atz$^-$ ligands in **1** grow almost in one direction (along the *c*-axis direction) due to the N–H…O hydrogen bonding interactions.

3.3. Crystal structure of complex 2

The asymmetric unit of compound **2** contains one Zn(II) cation, one crystallographically independent anionic atz$^-$, one coordinated isonic$^-$ ligand and one isolated disorder Hisonic molecule, respectively. The coordination environment of the Zn atom is similar to that in complex **1**, where the four-coordinated Zn atom adopts a tetrahedral geometry (Fig. 2a). The isonic$^-$ anion and the atz$^-$ anion adopt monodentate μ_2-bridge coordination modes (Chart 1b and d) to link two Zn atoms, respectively, and each Zn atom is surrounded by two atz$^-$ ligands and two isonic$^-$ ligands. The Zn–O_{isonic} bond length is 1.948(2) Å). The Zn–N_{atz} bond lengths are 1.975(3) and 1.992(3) Å, respectively. The mean Zn–N_{atz} bond length (1.988(3) Å) is slightly shorter than that of Zn–N_{isonic} (2.044(2) Å). All the Zn–N or Zn–O bond lengths are comparable to those previously reported Zn(II)–tetrazole complex [20,24,26,39], and the Zn(II)–isonic complex. The cis-angles at the central Zn atom fall in range of 107.0(1)–120.6(1)°, indicating that the tetrahedral geometries are slightly distorted.

In complex **2**, the tetrahedrally coordinated Zn atoms are connected by the μ_2-isonic$^-$(N,O) ligand into a zigzag chain (Fig. 2b) along the [101] direction, then the zigzag chains are further linked to other four zigzag chains by four μ_2-atz$^-$ ligands in four directions to form a 3D porous framework (Fig. 2c). Interestingly, there exist weak zigzag H-bond chains formed by the amino groups and the carboxylate oxygen atoms (N1–H2…O2(♯4), 3.010 Å, O1–H1…N1, 3.060 Å), along the [101] direction in **3** (Figure S2). These zigzag H-bond chains will be beneficial to the stabilization of the structure of **3**. Taking Zn1 atoms as nodes, the connections representing isonic$^-$ and atz$^-$ anions, the single 3D framework can be described as a 4-connected 3D topological network, with the short (Schläfli) vertex symbol [37] of 6^6 and the long topological (O'Keeffe) vertex symbol [38] of $6_2\cdot6_2\cdot6_2\cdot6_2\cdot6_2\cdot6_2$, which is a typical diamondoid network (Fig. 2d). Inspection of Figure S3 reveals large channels with a hexagonal cross section. These intraframework voids are partly occupied by a second identical network. In other words, the two identical 6^6 nets are further interpenetrated in 2-fold mode (Fig. 2e). Notably, many interpenetration structures have been reported to date, it has been considered that the interpenetration structure is not consistent with the creation of porous structures because the cavities are usually occupied by the self-including structure [40–45]. Remarkably, even if the interpenetration occurs in complex **2**, it still creates microporous channels with dimensional of about 3×5 Å^2 (after exclusion of the van der Waals radii of the surface atoms), filled with disorder Hisonic molecules along the [101] direction (Fig. 2f, Figure S4).

It should be emphasized that complex **1** and **2** are obtained from the similar condition except the second ligands Hnic and Hisonic are different but they are position-isomer ligands. However, little difference results into distinct features of the complexes. The reason for the two different structures is that the ligands nic and isonic have the difference in the coordination orientation of the two binding sites, py and carboxylate groups, straight for isonic, and bent for nic. The nic is bent and thus compensates for the tetrahedral Zn, and thus a 2D (4,4) sheet is formed. The isonic ligand, however, is linear, and so the tetrahedral geometry of the Zn then directs the formation of a 3D net with tetrahedral nodes. In other words, in complex **1**, the linear chains were connected by atz$^-$ ligand in two different directions (Fig. 1b), so complex **1** is a simple 2D square lattice structure. Whereas complex **2** possessed a zigzag chain (Fig. 2b), the Zn atoms in the zigzag chain linked to other four identical chains by the atz$^-$ ligand in four directions, and then construct a 3D framework with free Hisonic locating in the channels.

3.4. Crystal structure of complex 3

Single crystal X-ray analysis shows that complex **3** is a non-interpenetrating 3D framework. It crystallizes in orthorhombic space group *Pbcm*. The asymmetric unit of complex **3** contains half crystallorgraphically independent Cd(II) atom, half of a isonic ligand and a half atz ligand, respectively. The Cd center lies on a crystallorgraphic 2-fold axis and coordinated with three nitrogen atoms from two different atz$^-$ ligands (N3 and N3(i)) and one isonic ligand (N1(iv)), four oxygen atoms (O1, O1(ii) and O1(iii)) from the three different isoinic ligands to form a octahedron (Fig. 3). The equatorial plane of N3–O1(ii)–N(i)–O1(iii) is slightly distorted. The bond length of Cd$-N_{atz^-}$ in the equatorial plane is 2.254(3) Å, which is close to those reported for the Cd–N complex [23,46], while the bond lengths of Cd$-N_{isonic^-}$ (2.504(4) Å) on the axially ligated isonic ligand is little longer than the usual value. The Cd$-O_{isonic^-}$ bond lengths (Cd–O1 = 2.635(3) Å, Cd–O1(ii) = 2.419(3) Å) are slightly longer than normal, but are still in the range of those observed in the Cd/isonicotinate or nicotinate when the carboxylato group coordinate to the Cd atom by the μ_2,η^3-bridge fashion [46,47]. In complex **3**, the Cd atoms are linked into a double M–O–M (metal–oxygen–metal) chains by the μ_2, η^4-carboxylato groups along the *b*-axis direction. The neighboring double M–O–M chains are associated by the pyridyl ring spacer to provide a 2D layer, parallel to the (001) plane (Fig. 3b). The adjacent 2D layers are connected by the μ_2-atz bridging ligands into a three-dimensional pillared-layer structure (Fig. 3c). The 3D pillared-layer structure are further stabilized by the weak intralayer N–H…O hydrogen bonding interactions (N2–H2…O1(♯3), 2.954 Å), *via* the amino groups donating H atoms to the carboxylate oxygen atoms.

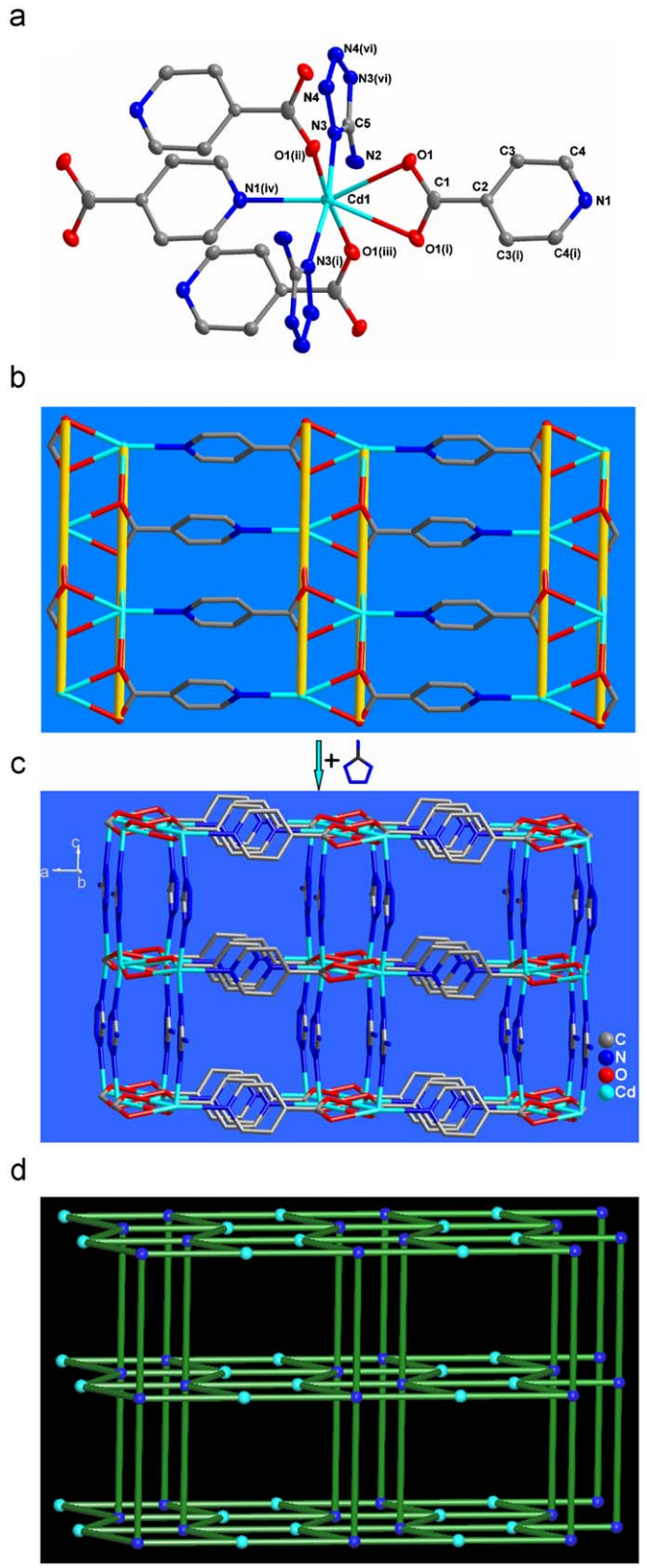

Fig. 3. (a) View of the coordination environment of Cd^{2+} in complex **3** at 50% probability level with labeling schedule. Hydrogen atoms are omitted. Symmetry codes: (i) x, $0.5-y$, $1-z$; (ii) $-x$, $-y$, $1-z$; (iii) $-x$, $0.5+y$, z; (iv) $1+x$, y, z and (vi) x, y, $0.51-z$. (b) Single 2D framework constructed from the double M–O–M chains and the pyridyl ring spacers. (c) View of the 3D framework in **3** formed by the pillared atz ligand along the bc plane. The hydrogen atoms are omitted for clarity. Color code: blue = N; gray = C; red = O; cyan = Cd. (d) View of the 3D (4,6)-connected topological network with the Schläfli symbol of $(4^4\cdot6^2)(4^4\cdot6^{10}\cdot8)$ network for complex **3**. Cd and isonic nodes are represented by blue and cyan balls, respectively. (For interpretation of the references to color in this figure legend, the reader is referred to the web version of this article.)

Topologically, each isonic ligand is connected to four adjacent Cd centers through three Cd–O bonds and one Cd–N bond, and each Cd^{2+} ion links with four isonic ligands and two atz ligands. Thus, the isonic ligand and Cd^{2+} ion can be defined as a 4- and 6-connected node and the μ_2-bridging atz ligand can be consider as linker between two 6-connected nodes. Based on this simplification, the structure of **3** can be described as a (4,6)-connected "*fsc*" topological network [48], with the short (Schläfli) vertex symbol [37] of $(4^4\cdot6^2)(4^4\cdot6^{10}\cdot8)$ and the long topological (O'Keeffe) vertex symbol [38] of $(4\cdot4\cdot4\cdot4\cdot6_2\cdot6_2)(4\cdot4\cdot4\cdot4\cdot6_5\cdot6_5\cdot6_5\cdot6_5\cdot6_5\cdot6_5\cdot{}^*\cdot{}^*\cdot{}^*)$ (Fig. 3d). It is a rarely observed topological net in coordination polymers. Although a few (4,6)-connected networks with two types of vertexes have been identified and categorized by O'Keeffe et. al., structures containing "*fsc*" topological network has been reported rarely. To the best of our knowledge, only one complex with *fsc*-type topology predicted by O'Keeffe in theory has been reported [49].

Compared with complex **2**, larger Cd atom radius and variable coordination number versus the Zn atom result into two distinct 3D networks. In complex **3**, more coordination numbers of Cd atom need more coordination atom to coordinate with it, so the coordination number of Cd atom was completed by sharing the O atoms of the carboxyl and results into a Cd–COO^-–Cd double chains, and then formed a "*fsc*" topological network through the μ_2-atz bridging ligand. In complex **2**, the tetrahedrally coordinated Zn atoms are completed by the N and O atoms of the isonic or atz ligand and formed zigzag chains, and then the chains were connected into a 2-fold interpenetrating 3D framework by the bridging atz ligand.

3.5. IR spectroscopy

The IR spectra of complexes **1**–**3** (see Figure S5, Supporting information), show the characteristic bands of the carboxylic groups in the usual region at 1392–1449 cm^{-1} for the symmetric vibrations and at 1619–1625 cm^{-1} for the asymmetric vibrations. The absence of the peak around 1661 cm^{-1}, which is observed in the starting Hnic or Hisoinc material, indicates that all carboxyl groups of organic moieties in **2** are deprotonated. The complexes show several strong band in the range of 3202–3417 cm^{-1}, which can be assigned to the ν(NH) stretching frequency of the NH_2 group [14]. In the range of 994–1087 cm^{-1} many deformation vibrations and combinations of the tetrazole ring can be found.

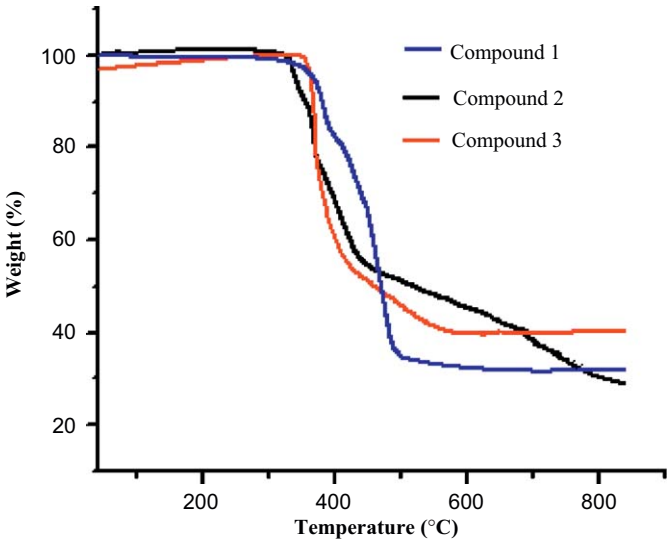

Fig. 4. TGA diagrams of complexes **1**, **2** and **3**.

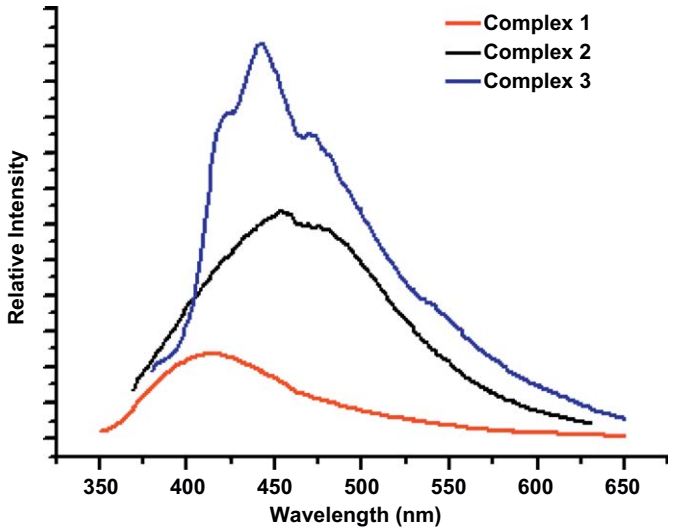

Fig. 5. Solid-state fluorescence spectra of **1** ($\lambda_{em} = 410$ nm), **2** ($\lambda_{em} = 455$ nm) and **3** ($\lambda_{em} = 442$ nm) at room temperature.

3.6. Thermal stability analyses

The thermal stability of the complexes in N_2 were examined by the TG techniques in the temperature range of 40–900 °C. Fig. 4 shows the TG curves for complex **1**–**3** at a heating rate of 10 °C/min under N_2 atmosphere. As shown in Fig. 4, there is no weight loss before 320 °C. A sharp weight loss for **1** and **3** occurred about the temperature range of 320.0–550.0 °C (for **1**: obsd, 69.13%, calcd, 70.03%; for **3**: obsd, 60.08%, calcd, 59.70%) corresponding to the release of the atz and nic (isonic for **3**) ligands. In the wide temperature range of 320–800 °C, weight loss of 76.02% was observed for **2**, which is attributed to the departure of Hisonic free molecules and the release of the atz and isonic ligands (calcd: 75.06). Finally, the probable residua are metal-oxide from the calculating value of the weight loss.

3.7. Fluorescent properties

The solid-state fluorescent properties of the complexes were investigated at room temperature. As illustrated in Fig. 5, upon excitation of these solid samples at $\lambda = 340$ nm, the intense broad emission bands at 410 nm for **1**, 455 nm for **2**, 442 nm for **3**, are observed. For excitation wavelengths between 280 and 480 nm, there is no obvious emission observed for the free Hisonic ligand under the same experimental conditions, while free Hatz ligand presents a weak photoluminescence emission at 325 nm according to the reported literature. Therefore, the fluorescent emission of **2** and **3** may be proposed to originate from the coordination of isonic$^-$ to the Zn and Cd atom (ligand-to-metal charge transition, LMCT). Further compared with complex **2**, the emission of complex **3** becomes stronger, which is probably due to the differences of the metal ions. The density of electron cloud for oxygen atoms and the nitrogen atoms may be changed by the coordination of the metal ions [50–54]. The free Hnic exhibit fluorescent emission bands at 379 and 512 nm ($\lambda_{ex} = 330$ nm). Taking the emission bands of these free organic ligands into consideration, the emissions of **1** may also be assigned as ligand-to-metal charge transition (LMCT). Complexes **1**–**3** are air-stable and insoluble in water and common organic solvents. These coordination polymers may be excellent candidates for potential photoactive materials because they are highly thermally stable.

4. Conclusion

In summary, we have successfully applied mixed-ligand to construct three new coordination polymers with the second pyridylcarboxylate ligand and the *in situ* generated ligand of 5-amino-tetrazolate. Distinct spatial structural features in complex **1** and **2** were result from the position-isomer ligand. Simple "*sql*" topological 2D wave layers were connected into a 3D supramolecular structure via weak $\pi \ldots \pi$ stacking interaction for **1**. Interpenetrated 3D framework of **2** with 1D channel was constructed by the *in situ* generated bridging atz ligand and the bridging isonic ligand, non-interpenetrated 3D framework of **3** with a rarely observed "*fsc*" topology. These results reveal that the mixed-ligand synthetic approach is reliable to achieve unusual MOFs in tetrazole-based system. From the investigation of the fluorescent properties, complexes **1**–**3** may be potential blue fluorescence material. The further investigations on such an interesting system are still in progress.

Supporting information

X-ray crystallographic data in CIF format, IR spectra for complexes **1**–**3**, and additional figures for **1** and **2**. Crystallographic data have been deposited with the Cambridge Crystallographic Data Centre, CCDC nos. 721436,721437 and 721438 for complexes **1**, **2** and **3**, respectively. Copies of this information may be obtained free of charge from The Director, CCDC, 12 Union Road, Cambridge, CB2 1EZ, UK (fax: +44 1223 336 033; e-mail: deposit@ccdc.cam.ac.uk or www: http://www.ccdc.cam.ac.uk).

Acknowledgments

This work was supported by the National Natural Science Foundation of China (50772023), the Natural Science Foundation of Fujian Province (2007J0148), the open fund of National Photonic Crystal Materials Engineering and Technology Research Centre (07h3561xaa), the Education Foundation of Fujian Province (JB06049), and the Innovation Fund for Yong Scientist of Fujian Province (2008F3059).

Appendix A. Supplementary material

Supplementary data associated with this article can be found in the online version at doi:10.1016/j.jssc.2009.04.034.

References

[1] H. Zhao, Z.R. Qu, H.Y. Ye, R.G. Xiong, Chem. Soc. Rev. 37 (2008) 84–100.
[2] P.N. Gaponik, S.V. Voitekhovich, O.A. Ivashkevich, Russ. Chem. Rev. 75 (2006) 507–539.
[3] P.E.M. Wijnands, J.S. Wood, J. Reedijk, W.J.A. Maaskant, Inorg. Chem. 35 (1996) 1214–1222.
[4] A. Ozarowski, B.R. McGarvey, Inorg. Chem. 28 (1989) 2262–2266.
[5] Y. Shvedenkov, M. Bushuev, G. Romanenko, L. Lavrenova, V. Ikorskii, P. Gaponik, S. Larionov, Eur. J. Inorg. Chem. (2005) 1678–1682.
[6] K.K. Palkina, N.E. Kuz'mina, A.S. Lyakhov, P.N. Gaponik, A.N. Bogatikov, A.A. Govorova, L.S. Ivashkevich, Russ. J. Inorg. Chem. 46 (2001) 1649–1651.
[7] A.V. Virovets, N.V. Podberezskaya, L.G. Lavrenova, G.A. Bikzhanova, Polyhedron 13 (1994) 2929–2932.
[8] A.F. Stassen, H. Kooijman, A.L. Spek, L.J. de Jongh, J.G. Haasnoot, J. Reedijk, Inorg. Chem. 41 (2002) 6468–6473.
[9] A.F. Stassen, E. Dova, R. Ensling, H. Schenk, P. Gutlich, J.G. Haasnoot, J. Reedijk, Inorg. Chim. Acta 335 (2002) 61–68.
[10] E. Dova, R. Peschar, M. Sakata, K. Kato, H. Schenk, Chem. Eur. J. 12 (2006) 5043–5052.

[11] A.F. Stassen, M. Grunert, A.M. Mills, A.L. Spek, J.G. Haasnoot, J. Reedijk, W. Linert, Dalton Trans. (2003) 3628–3633.
[12] Z.P. Demko, K.B. Sharpless, J. Org. Chem. 66 (2001) 7945–7950.
[13] Z.P. Demko, K.B. Sharpless, Angew. Chem. Int. Ed. 41 (2002) 2110–2113.
[14] Y.-L. Yao, L. Xue, Y.-X. Che, J.-M. Zheng, Cryst. Growth Des. 9 (2009) 606–610.
[15] A. Rodriguez-Dieguez, M.A. Palacios, A. Sironi, E. Colacio, Dalton Trans. (2008) 2887–2893.
[16] L.L. Zheng, H.X. Li, J.D. Leng, J. Wang, M.L. Tong, Eur. J. Inorg. Chem. (2008) 213–217.
[17] X.Q. Zhang, Q. Yu, H.D. Bian, S.P. Yan, D.Z. Liao, W. Gu, H. Liang, Aust. J. Chem. 61 (2008) 303–309.
[18] W.W. Dong, J. Zhao, L. Xu, J Solid State Chem. 181 (2008) 1149–1154.
[19] H. Deng, Y.C. Qiu, Y.H. Li, Z.H. Liu, R.H. Zeng, M. Zeller, S.R. Batten, Chem. Commun. (2008) 2239–2241.
[20] X.W. Wang, J.Z. Chen, J.H. Liu, Cryst. Growth Des. 7 (2007) 1227–1229.
[21] R.S. Yathirajan, M. Nethaji, B. Prabhuswamy, C.R. Raju, P. Nagaraja, S. Shashikanth, M.N. Ponnuswamy, K. Palani, Cryst. Res. Technol. 41 (2006) 299–303.
[22] T. Wu, R. Zhou, D. Li, Inorg. Chem. Commun. 9 (2006) 341–345.
[23] X. He, C.Z. Lu, D.Q. Yuan, Inorg. Chem. 45 (2006) 5760–5766.
[24] X.S. Wang, Y.Z. Tang, X.F. Huang, Z.R. Qu, C.M. Che, P.W.H. Chan, R.G. Xiong, Inorg. Chem. 44 (2005) 5278–5285.
[25] X. Xue, X. Wang, L.Z. Wang, R.G. Xiong, B.F. Abrahams, X.Z. You, Z.L. Xue, C.M. Che, Inorg. Chem. 41 (2002) 6544–6546.
[26] X. Xue, B.F. Abrahams, R.G. Xiong, X.Z. You, Aust. J. Chem. 55 (2002) 495–497.
[27] H. Ren, T.-Y. Song, J.-N. Xu, S.-B. Jing, Y. Yu, P. Zhang, L.-R. Zhang, Cryst. Growth Des. 9 (2009) 105–112.
[28] Y.-Y. Lin, Y.-B. Zhang, J.-P. Zhang, X.-M. Chen, Cryst. Growth Des. 8 (2008) 3673–3679.
[29] M. Du, X.J. Jiang, X.J. Zhao, Chem. Commun. (2005) 5521–5523.
[30] M. Du, X.J. Jiang, X.J. Zhao, Inorg. Chem. 45 (2006) 3998–4006.
[31] X.J. Gu, D.F. Xue, Inorg. Chem. 45 (2006) 9257–9261.
[32] M.B. Zhang, J. Zhang, S.T. Zheng, G.Y. Yang, Angew. Chem. Int. Ed. 44 (2005) 1385–1388.
[33] J.W. Cheng, J. Zhang, S.T. Zheng, M.B. Zhang, G.Y. Yang, Angew. Chem. Int. Ed. 45 (2006) 73–75.
[34] Y.S. Song, B. Yan, Z.X. Chen, J Solid State Chem. 179 (2006) 4037–4046.
[35] Y.H. Zhao, Z.M. Su, Y. Wang, Y.M. Fu, S.D. Liu, P. Li, Inorg. Chem. Commun. (2007) 410–414.
[36] G.M. Sheldrick, SHELXS-97, Program for Crystal Structure Refinement, University of Göttingen, Germany, 1997.
[37] J.V. Smith, Am. Min. 63 (1978) 960.
[38] M. O'keeffee, S.T. Hyde, Zeolites 19 (1997) 370.
[39] M. Dinca, A.F. Yu, J.R. Long, J. Am. Chem. Soc. 128 (2006) 8904–8913.
[40] D. Hagrman, R.P. Hammond, R. Haushalter, S. Zubieta, J. Chem. Mater. 10 (1998) 2091.
[41] G.B. Gardner, D. Venkataraman, J.S. Moore, J.S. Lee, Nature 374 (1995) 792.
[42] B.F. Hoskins, R. Robson, J. Am. Chem. Soc. 112 (1990) 1546–1554.
[43] O.M. Yaghi, G.M. Li, Angew. Chem. Int. Ed. Engl. 34 (1995) 207–209.
[44] O.M. Yaghi, H. Li, J. Am. Chem. Soc 118 (1996) 295–296.
[45] L.R. MacGillivray, S. Subramanian, M.J. Zaworotko, J. Chem. Soc. Chem. Commun. (1994) 1325–1328.
[46] O.R. Evans, Z. Wang, R.G. Xiong, B.M. Foxman, W. Lin, Inorg. Chem. 38 (1999) 2969–2973.
[47] O.R. Evans, W. Lin, Chem. Mater. 13 (2001) 3009–3017.
[48] A.F. Wells, Three-dimensional Nets and Polyhedra, Wiley, New York, 1977.
[49] M. Bi, G. Li, J. Hua, Y. Liu, X. Liu, Y. Hu, Z. Shi, S. Feng, Cryst. Growth Des. 7 (2007) 2066–2070.
[50] S.K. Kurtz, T.T. Perry, J. Appl. Phys. 39 (1968) 3798–3813.
[51] C.M. Che, C.W. Wan, K.Y. Ho, Z.Y. Zhou, New J. Chem. 25 (2001) 63.
[52] H. Yersin, A. Vogler, Photochemistry and Photophysics of Coordination Compounds, Springer, Berlin, 1987.
[53] B. Valeur, Molecular Fluorescence: Principles and Applications, Wiley-VCH, Weinheim, 2002.
[54] A.W. Adamson, P.D. Fleischauer, Concepts of Inorganic Photochemistry, Wiley, New York, 1975.